Supplement of Weather Clim. Dynam., 3, 471–482, 2022
https://doi.org/10.5194/wcd-3-471-2022-supplement

Supplement of

Extreme Atlantic hurricane seasons made twice as likely by ocean warming

Peter Pfleiderer et al.

Correspondence to: Peter Pfleiderer (peter.pfleiderer@climateanalytics.org)

Contents

S1 Weather patterns

S1.1 Weights of weather patterns

S1.1.1 Figure S1: MSLP maps for the 20 weather patterns

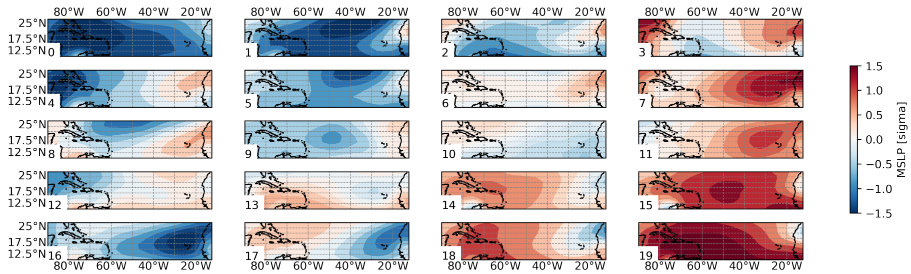

Figure S1: Mean sea level pressure (MSLP) anomalies for the 20 weather patterns expressed in standard deviations.

S1.1.2 Figure S2: VWS maps for the 20 weather patterns

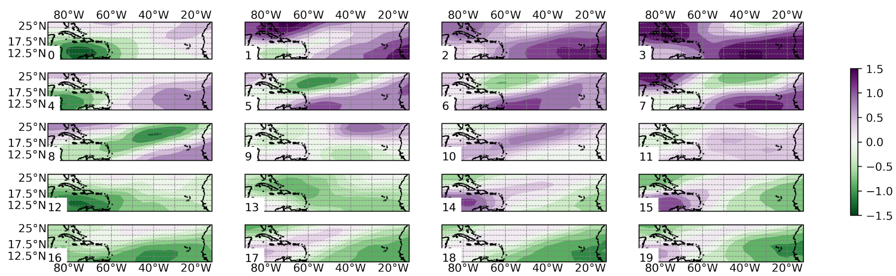

Figure S2: Vertical wind shear (VWS) anomalies for the 20 weather patterns expressed in standard deviations.

S1.2 TC activity in weather patterns

S1.2.1 Figure S3: TC statistics for the 20 weather patterns

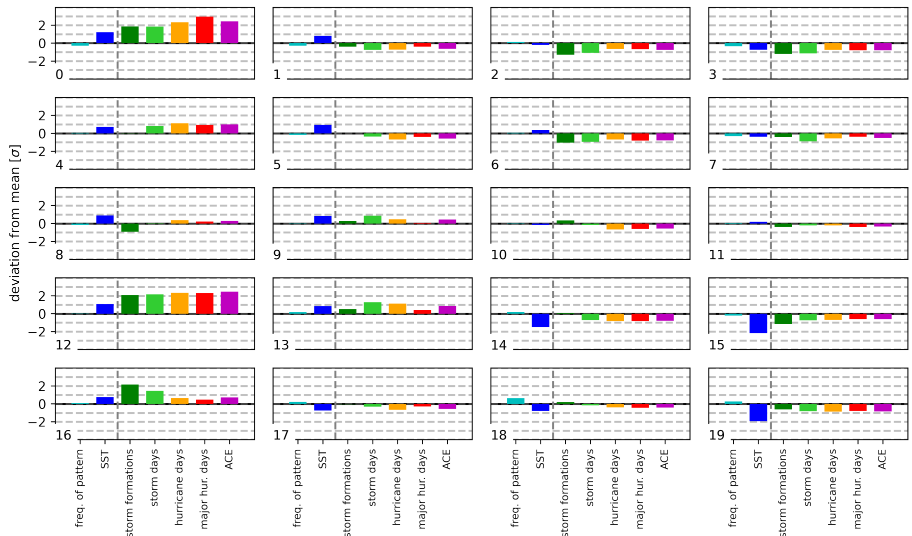

Figure S3: Tropical storm statistics for the 20 weather patterns expressed as relative deviations from the average.

S1.2.2 Figure S4: Storm formation locations in weather patterns

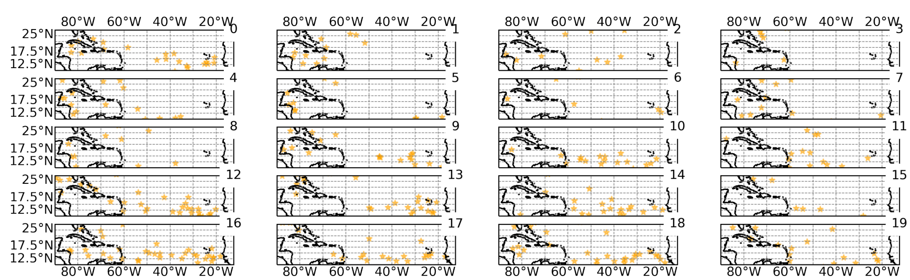

Figure S4: Storm formation locations for each weather pattern.

S1.2.3 Figure S5: Histograms of storm durations

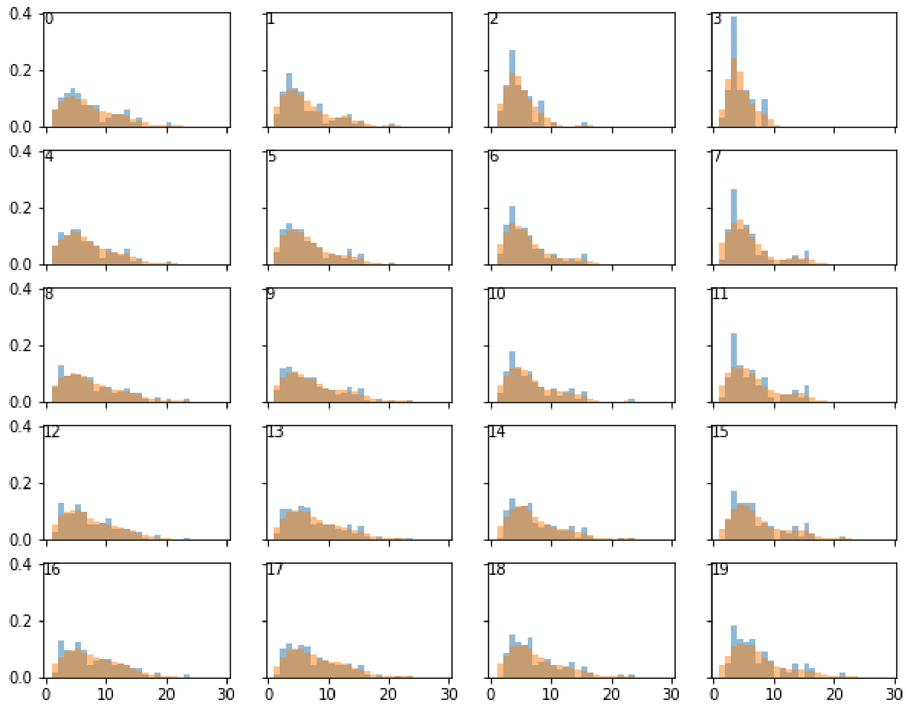

Figure S5: Histograms of observed storm durations of all storms that formed during each weather pattern (blue). The orange histograms show the distributions from which storm durations are sampled in the emulator.

S2 Sea surface temperatures (SST)

S2.1 Figure S6: Main development region (MDR)

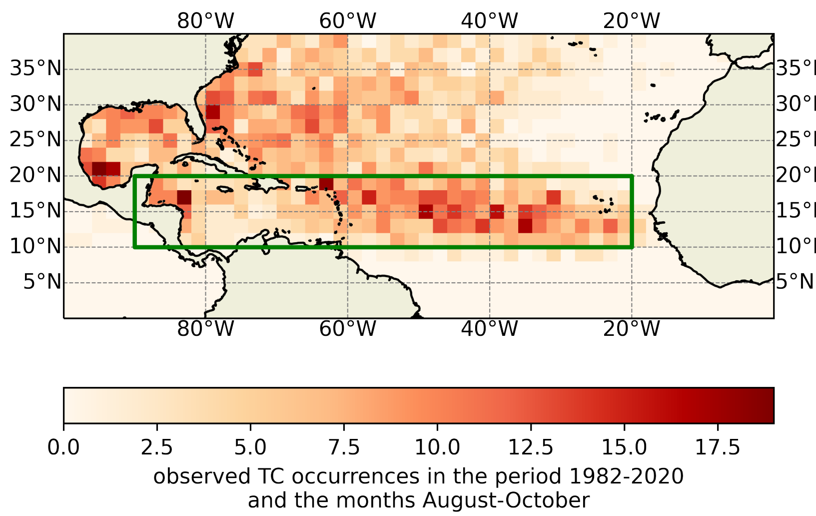

Figure S6: TC occurrences for the period 1982-2020 and the months August-October. The main development region (MDR) is indicated by a green rectangle and spans the area 90W-20W and 10N-20N.

S2.2 Figure S7: Quantile regression SST vs TC intensity

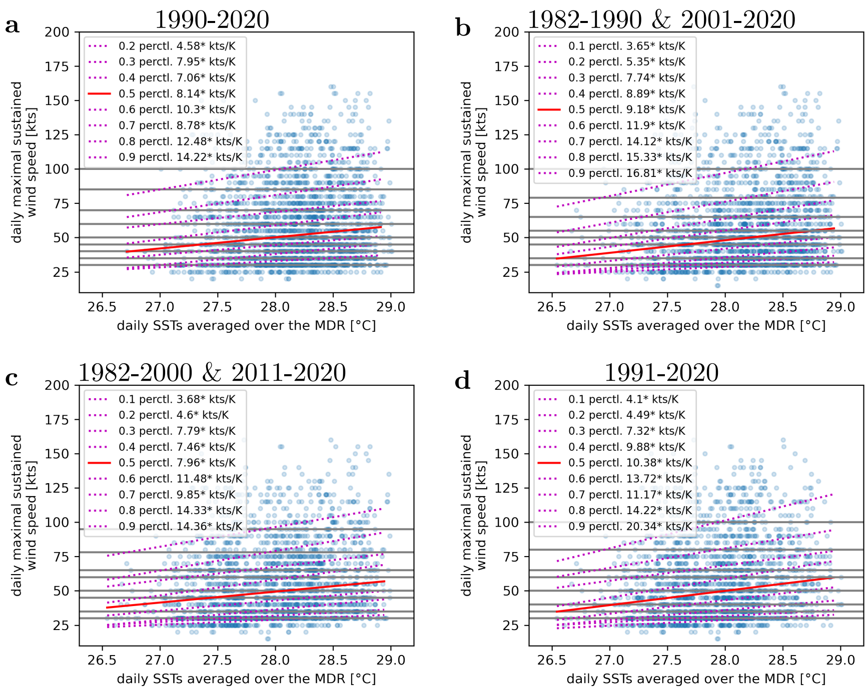

Figure S7: Quantile regression between daily maximal sustained wind speeds of tropical storms and daily SSTs averaged over the MDR. Quantiles for which the null-hypothesis of no trend can be rejected with a 95% confidence level are indicated by a star.

S2.3 Table S1: CMIP6 historical simulations - model list

We construct a CMIP6 historical ensemble by selecting on simulation run from each of the following models:

ACCESS-CM2, ACCESS-ESM1-5, AWI-CM-1-1-MR, AWI-ESM-1-1-LR, BCC-CSM2-MR, BCC-ESM1, CAMS-CSM1-0, CAS-ESM2-0, CESM2, CESM2-FV2, CESM2-WACCM, CESM2-WACCM-FV2, CIESM, CMCC-CM2-HR4, CMCC-CM2-SR5, CMCC-ESM2, CNRM-CM6-1, CNRM-CM6-1-HR, CNRM-ESM2-1, CanESM5, CanESM5-CanOE, E3SM-1-0, E3SM-1-1, E3SM-1-1-ECA, EC-Earth3, EC-Earth3-AerChem, EC-Earth3-CC, EC-Earth3-Veg, EC-Earth3-Veg-LR, FGOALS-f3-L, FGOALS-g3, FIO-ESM-2-0, GFDL-CM4, GFDL-ESM4, GISS-E2-1-G, GISS-E2-1-G-CC, GISS-E2-1-H, HadGEM3-GC31-LL, HadGEM3-GC31-MM, ICON-ESM-LR, IITM-ESM, INM-CM4-8, INM-CM5-0, IPSL-CM5A2-INCA, IPSL-CM6A-LR, KACE-1-0-G, KIOST-ESM, MCM-UA-1-0, MIROC-ES2L, MIROC6, MPI-ESM-1-2-HAM, MPI-ESM1-2-HR, MPI-ESM1-2-LR, MRI-ESM2-0, NESM3, NorCPM1, NorESM2-LM, NorESM2-MM, SAM0-UNICON, TaiESM1, UKESM1-0-LL

Table S1: Models used to estimate the forced trend in MDR SSTs over the period 1982-2014

S3 Sensitivity analysis

For each of the emulator components heuristic methodological decision had to be taken. In the following we show how the emulator performs compared to alternative methodological choices.

S3.1 Storm formations

S3.1.1 Simplest approach - fig S8b

The probability for a new storm is the number of storm formations during the weather pattern $w(d)$ of the day d that is emulated divided by the number of observed days with that weather pattern:

$$P_{gen}(d) = P_{obs}(gen|w(d)) \tag{1}$$

S3.1.2 Giving more weight to the weather history - fig S8c

As in the main component, the probability of finding a storm formation is multiplied by the probabilities of finding a storm formation on the following day of the weather pattern of the day before and respectively two days before. In contrast to the main component, these additional probability factors are not normalised by dividing by the overall observed genesis probability squared.

$$P_{gen}(d) = P_{obs}(gen|w(d)) * \frac{P_{obs}(gen_{next\ day}|w(d-1)) * P_{obs}(gen_{2\ days\ after}|w(d-2))}{P_{obs}(gen|all)^2} \tag{2}$$

S3.1.3 Nearest neighbours with weather pattern and SST - fig S8d

For each combination of SST and weather pattern, the 100 nearest neighbours in the observations are taken and the genesis probability is estimated from these observations.

We use the Euclidean distance metric and standardise our variables for the distance calculation.

$$D(d_i, d_j)^2 = \frac{(SST(d_i) - SST(d_j))^2}{\sqrt{\frac{1}{N}\sum_m (SST(d_m) - \overline{SST})^2}} + \frac{(w(d_i) - w(d_j))^2}{\sqrt{\frac{1}{N}\sum_m (w(d_m) - \overline{w})^2}} \tag{3}$$

For the weather patterns, which are not a continuous variable, we consider their coordinates in the SOM grid as locations and calculate differences between weather patterns as the sum of the squared differences in row and column numbers.

$$w(d_i) - w(d_j) = \sqrt{(w_{row}(d_i) - w_{row}(d_j))^2 + (w_{col}(d_i) - w_{col}(d_j))^2} \tag{4}$$

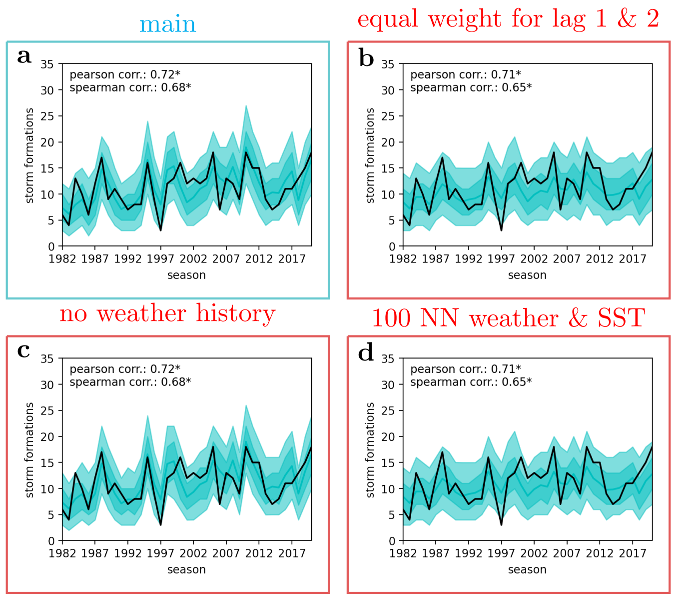

Figure S8: Seasonal storm formation counts for the main storm formation component (a), an alteration where more weight is given to the weather history (b), an alternation where the weather history is ignored (c) and an alteration where storm formations are sampled using a nearest neighbors approach based on SSTs and weather patterns (d). The black line indicates the observed storm counts. The solid cyan line shows the mean of 1000 cross-validated simulations. The light shading shows the 95% range of the 1000 simulations, the darker shading shows the 66% range.

All storm formation components result in similarly high correlation coefficients between the hindcasted emulations and the observed numbers of storm formations. Including the information of weather patterns on the two days before makes the component more sensitive while without this information the emulations remain close to the long-term mean.

S3.2 Storm duration

S3.2.1 No averaging over neighboring weather patterns - fig S9b

The length of a storm is sampled from the probability function of all storms that emerged during the same weather pattern:

$$D(s) = f_g(D_{obs}[w = w(d_f)]) \tag{5}$$

S3.2.2 Independent of weather patterns - fig S9c

The duration of a storm is sampled from the probability distribution of all observed storms:

$$D(s) = f_g(D_{obs}) \tag{6}$$

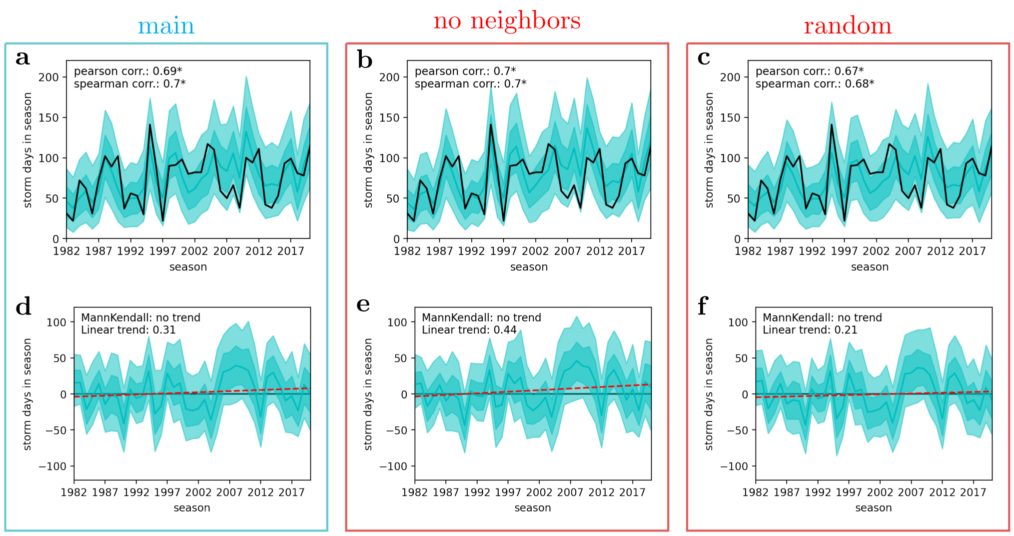

Figure S9: Seasonal storm day counts for the main storm formation component (a), an alteration where the durations are estimated from the current weather pattern without averaging over neighboring weather patterns (b), a storm formation component that samples from a distribution of all observed storm lengths (d). The black line indicates the observed storm counts. The solid cyan line shows the mean of 1000 cross-validated simulations. The light shading shows the 95% range of the 1000 simulations, the darker shading shows the 66% range. The second row shows the residuals of the simulations for the respective plots of the first row.

Variations between the three tested storm duration components are small.

S3.3 Storm intensity

S3.3.1 Nearest neighbours approach

The storm intensity is sampled from a 100 nearest neighbors distribution with conditions being characterized by weather patterns, SSTs and the storm intensity on the day before. This is a simpler variation of the main component that works without the quantile regression between storm strengths and SSTs.

$$\begin{aligned} D(d_i, d_j)^2 = & \frac{(SST(d_i) - SST(d_j))^2}{\sqrt{\frac{1}{N}\sum_m (SST(d_m) - \overline{SST})^2}} \quad + \frac{(w(d_i) - w(d_j))^2}{\sqrt{\frac{1}{N}\sum_m (w(d_m) - \overline{w})^2}} \\ & + \frac{(v(d_i - 1) - v(d_j - 1))^2}{\sqrt{\frac{1}{N}\sum_m (v(d_m) - \overline{v})}} \end{aligned} \tag{7}$$

The initial idea for this component of the emulator was this nearest neighbors approach. As shown in figure S10 there is not enough data to find close enough neighbors for all possible combinations of weather pattern, SST and intensities on the day before. This problem is most pronounced for strong storms under unfavorable weather conditions. Using 20 nearest neighbors instead of 100 only slightly improves this problem.

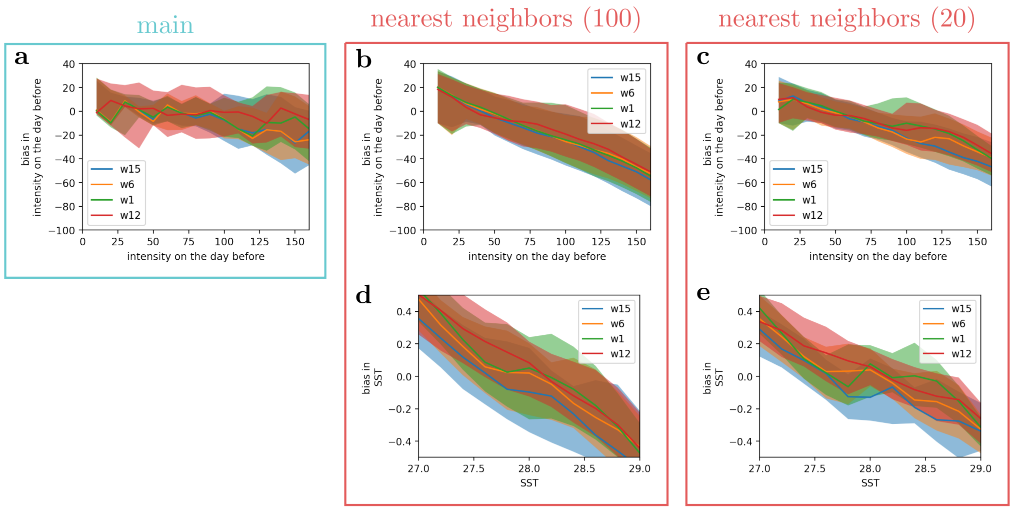

Figure S10: First row: Deviation from the storm intensity on the day before in the nearest neighbor observations for different requested storm intensities on the day before (x-axis). Second row: Deviation from the requested SST in the nearest neighbor observations for different requested SSTs (x-axis). Main emulator (a), 100 nearest neighbors (b,d), 20 nearest neighbors (c,e). The black line indicates the observed storm counts. The solid cyan line shows the mean of 1000 cross-validated simulations. The light shading shows the 95% range of the 1000 simulations, the darker shading shows the 66% range.

S3.3.2 No SST dependence

The storm intensity is sampled from a 100 nearest neighbors distribution with conditions being characterized by weather patterns and the storm intensity on the day before.

Building an emulator without any dependence on SSTs by simply using the 100 nearest neighbors in terms of weather patterns and storm histories leads to a similar performance in terms of year to year variability. However, there is a significant trend in the residuals of seasonal major hurricane counts that shows that the effect of warming SSTs in the region on TC activity cannot be reproduced without SSTs. As shown in figure S11d this trend is even more pronounced if seasonal major hurricane counts are plotted against the seasonally averaged SSTs.

The misrepresentation of major hurricanes leads to a considerable trend in ACE residuals (fig. S12).

Note that there is a positive trend in the residuals of simulated storm days which could propagate into major hurricane counts and ACE.

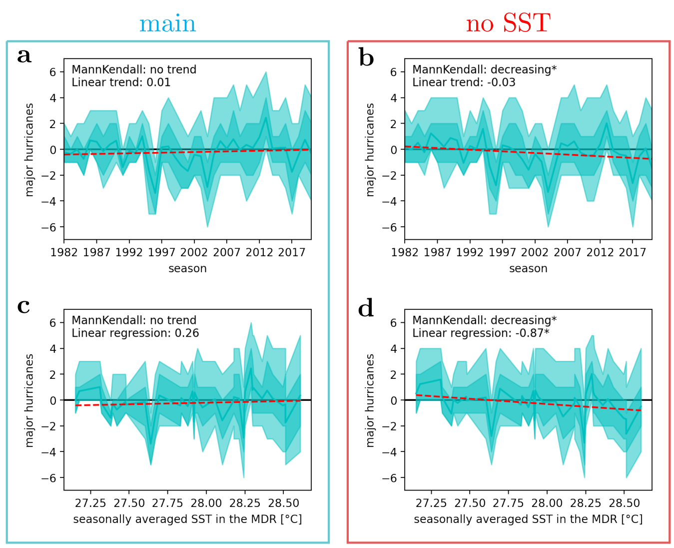

Figure S11: Residuals in seasonal major hurricane counts in the main emulator (a) and an emulator without SST dependence (b). Panels (c-d) show the same, but against the seasonally averaged SSTs in the MDR instead of years. The black line indicates the observed storm counts. The solid cyan line shows the mean of 1000 cross-validated simulations. The light shading shows the 95% range of the 1000 simulations, the darker shading shows the 66% range.

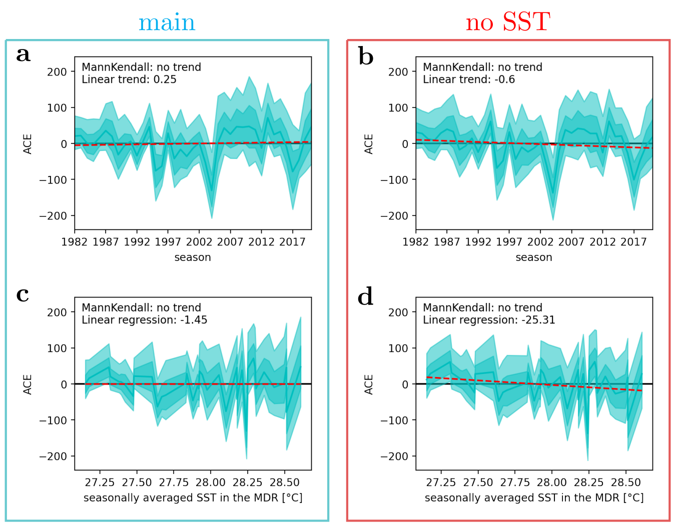

Figure S12: Residuals in seasonal major hurricane counts in the main emulator (a) and an emulator without SST dependence (b). Panels (c-d) show the same, but against the seasonally averaged SSTs in the MDR instead of years. The black line indicates the observed storm counts. The solid cyan line shows the mean of 1000 cross-validated simulations. The light shading shows the 95% range of the 1000 simulations, the darker shading shows the 66% range.

S3.3.3 No weather dependence

Storm intensities are emulated as in the main component with the only difference, that the dependence on weather patterns is removed.

Removing the dependence of weather patterns on storm intensification only slightly alters the emulations. As shown in figure S13, with this variation there is a tendency towards fewer hurricane and major hurricane strength storms.

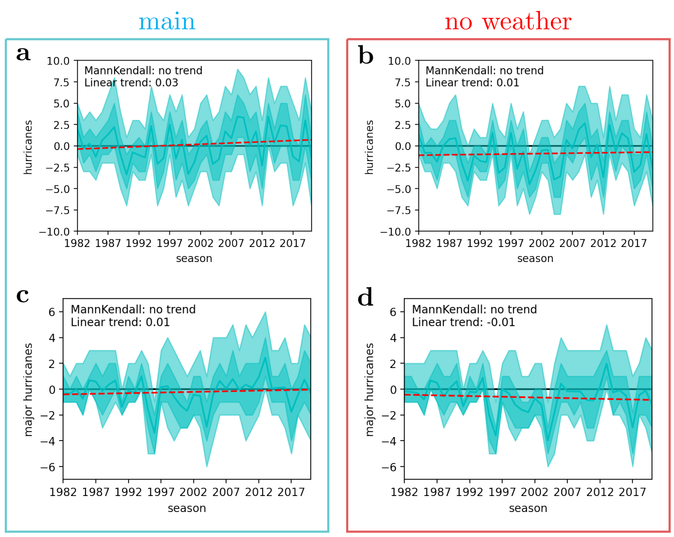

Figure S13: Residuals in seasonal hurricane (a-b) and major hurricane (c-d) counts in the main emulator (a,c) and an emulator without weather dependence (b,d). The black line indicates the observed storm counts. The solid cyan line shows the mean of 1000 cross-validated simulations. The light shading shows the 95% range of the 1000 simulations, the darker shading shows the 66% range.

S3.3.4 No storm memory

Storm intensities are emulated as in the main component with the only difference, that the dependence on the storm intensity on the day before is removed.

When intensities are estimate irrespective of the intensity of the storm on the day before the performance of the emulator is considerably poorer. As shown in figure S14 there are twice as many hurricanes and major hurricanes in the emulations than observed.

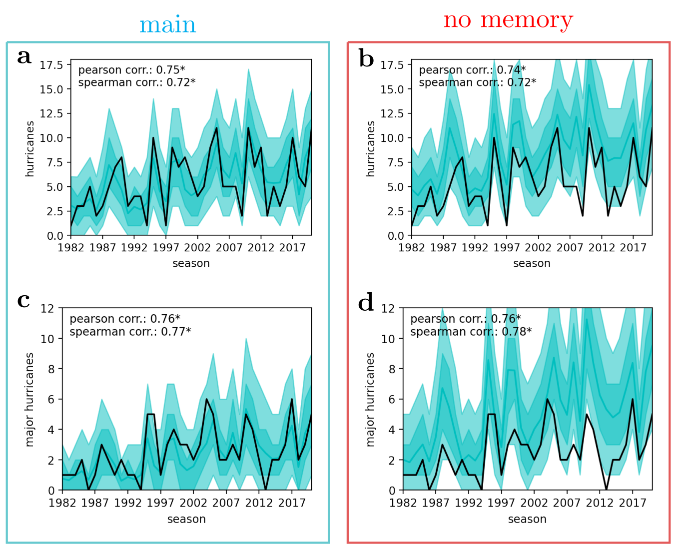

Figure S14: Seasonal hurricane (a-b) and major hurricane (c-d) counts in the main emulator (a,c) and an emulator without memory in the storm evolution (b,d). The black line indicates the observed storm counts. The solid cyan line shows the mean of 1000 cross-validated simulations. The light shading shows the 95% range of the 1000 simulations, the darker shading shows the 66% range.